Delay Mathematical Model of Chickenpox Disease with Vertical Transmission

TARIKU MERGA TOLASA*, HENOK DESALEGN DESTA, WORKU MIHRET FENTA
Department of Mathematics,
Haramaya University,
Dire Dawa,
ETHIOPIA

*Corresponding Author

Abstract: - The varicella-zoster virus (VZV) causes chickenpox, a highly transmissible airborne illness that predominantly affects children. Transmission occurs via respiratory droplets from infected individuals, as well as vertically from an infected mother to her fetus. After an incubation period of 10 to 21 days, patients typically present with fatigue, fever, and an itchy rash. The most robust prevention method is the two-dose measles, mumps, rubella, and varicella (MMRV) vaccine regimen. To better understand the dynamics of chickenpox, a delay differential mathematical model was developed. This model divides the entire population into six classes: susceptible $(\mathbf{S}(\mathbf{t}))$, vaccinated $(\mathbf{V}(\mathbf{t}))$, permanently immunized $(\mathbf{P}(\mathbf{t}))$, infected $(\mathbf{I}(\mathbf{t}))$, treated $(\mathbf{T}(\mathbf{t}))$, and individuals who have recovered $(\mathbf{R}(\mathbf{t}))$. The model factors in elements such as double doses of vaccine, incubation period, and vertical transmission, which significantly impact the dynamics of the disease. The analysis confirms that all solutions of compartments are positive, and the model is well-posed in the invariant region. The model's basic reproductive number ($\mathbf{R_0}$), computed using a next-generation matrix that was found to be $\mathbf{R_0 = 2.3234}$ with time delay and $\mathbf{R_0^d = 2.4742}$ without time delay. This result indicates that the endemic equilibrium point of the model is globally asymptotically stable and the reproductive number is less with a time delay as compared to the model without a time delay. The analysis included sensitivity analysis and numerical simulations, presented graphically using MATLAB 2019a software, to study the influence of key parameters. It was suggested that increasing the incubation period ($\boldsymbol{\tau}$), treatment rate ($\boldsymbol{\vartheta}$), first vaccination rate ($\boldsymbol{\alpha}$), and second vaccination rate ($\boldsymbol{\delta}$), as well as reducing the contact values rate ($\boldsymbol{\beta}$), and vertical transmission rate ($\boldsymbol{\theta}$), can help minimize the $\mathbf{R_0}$, leading to a reduced spread of chickenpox. Therefore, to effectively prevent and control the spread of chickenpox, it is important to understand the factors that increase its transmission and apply appropriate control strategies.

Key-Words: - chickenpox, incubation period, a delay differential equation, vertical transmission, basic reproductive number, double-dose, sensitive analysis and numerical simulation.

Received: April 7, 2026. Revised: May 9, 2026. Accepted: June 12, 2026. Published: November 12, 2026.

1 Introduction

Chickenpox is a highly contagious airborne viral infection caused by VZV [1]. The virus spreads through direct contact with contaminated objects, inhalation of contaminated air, or vertically from mother to fetus during pregnancy. Clinical symptoms usually manifest between 10 and 21 days post-exposure and persist for 5 to 7 days [2]. The disease is characterized by fatigue, fever, headaches, and a distinct itchy rash. While often mild in children, chickenpox can trigger severe complications in adults, such as pneumonia, encephalitis, and secondary bacterial skin infections [3]. Because of its rapid transmission, the disease continues to impose significant health and economic burdens, particularly in low-income regions [2], [4], [5], [6], [7], [8], [9] have highlighted the impact of chickenpox on children's health and economic crises in various countries, especially low-income countries.

To build community immunity, the MMRV vaccine is recommended in two doses [10]. While the first dose protects roughly 65% of recipients, this immunity wanes after 15 to 20 years. Complete,

lifelong protection requires the second dose. Although treatment helps manage symptoms and build immunity, the virus can remain dormant and later reactivate as shingles, typically affecting individuals over 50. Furthermore, VZV reactivates in up to one-third of infected individuals, especially those with aging immune systems [11].

Mathematical modeling is essential for understanding infectious disease dynamics and informing public health policy [12], [13]. These models convert complex biological interactions into actionable data for resource allocation [13], [14]. Specifically, delay differential equation (DDE) models are highly effective for capturing latent biological processes, such as incubation periods and the delayed effects of interventions [15], [16]. By incorporating time delays, researchers can more accurately assess the timing and efficacy of vaccination programs and maternal health protections [17]. This quantitative approach aligns with recent studies highlighting the value of mathematical models in policy planning [18]. For chickenpox, integrating delays related to transmission and vaccination is critical for predicting long-term prevalence and designing optimal immunization schedules.

By integrating time delay, these models enhance the evaluation of the timing and efficacy of disease control efforts, including vaccination programs and maternal health protection, for relevant stakeholders such as policymakers and health officials [17]. This viewpoint aligns with recent empirical studies emphasizing the use of quantitative modeling in decision-making. The study by [18] illustrated how mathematical models can guide policymaking by connecting system dynamics to practical planning requirements concerning residential water consumption and stated that, as evidence-based methodology is equally relevant to epidemiological modeling. In the context of chickenpox, it is crucial to incorporate delays related to transmission and vaccination programs for assessing long-term disease prevalence and for formulating optimal maternal health and immunization programs.

Numerous studies have used deterministic mathematical models to investigate the transmission dynamics of VZV, with particular emphasis on assessing the effectiveness of vaccination and other control interventions. For example, study [2] developed a mathematical model of chickenpox transmission that incorporated control measures to analyse disease dynamics. The authors derived the basic reproduction number (R_0) and examined the stability of equilibrium states to determine the conditions under which the disease could persist or be eliminated.

Based on this modelling framework, study [4] reinforced these findings by drawing upon existing epidemiological evidence and published literature, highlighting the significant role of vaccination in reducing disease transmission and burden. Extending the focus on vaccination strategies, study [5] investigated the impact of immunization programs through a mathematical model of chickenpox spread. In addition to deriving key epidemiological thresholds, the researchers performed sensitivity analyses to identify the parameters that most strongly influence R_0, thereby providing valuable insights for policymakers and public health stakeholders in designing effective control strategies. Similarly, study [6] emphasized the broader importance of mathematical modelling as a tool for understanding chickenpox transmission dynamics. Their findings further demonstrated how vaccination and immunization programs can mitigate disease spread, improve population-level protection, and contribute to the overall control of VZV within human communities.

The study by [19] focused on the occurrence and association of VZV, emphasizing its impact on a wide population. The purpose of this study was to better understand the transmission patterns of HIV and Zoster in co-infected persons, as well as to provide insights into successful interventions. These researchers claimed that VZV is a contagious virus that raises the likelihood of getting HIV/AIDS, and that reactivation frequently indicates the start of immunodeficiency. To understand the dynamics of co-infection between HIV and Zoster, this study used a mathematical model categorizing the population into seven groups: susceptible to both Zoster and HIV ($S(t)$), Zoster vaccinated class ($V(t)$), Zoster mono-infection class ($Z(t)$), HIV mono-infected class (($H(t)$), HIV and Zoster co-infection class ($C(t)$), Class of those with durably undetectable viral load ($D(t)$), and recovered class ($R(t)$). The study emphasized the importance of managing co-infections to reduce their impact on public health. In [20], the stability analysis of a reaction-diffusion model for Varicella virus transmission was examined. They utilized a reaction-diffusion SIQVR (susceptible, infected, quarantine, vaccination, and recovery compartments) spatiotemporal model to investigate

the spatiotemporal dynamics of Varicella-zoster virus transmission. The study presented a system of partial differential equations with Neumann boundary conditions to model the virus's evolution. It concluded that investigating nonlinear diffusion operators in an epidemic model is intriguing and that these operators could enhance the model's ability to comprehend intricate patterns and connections in the data.

Various authors have developed mathematical models to analyze the disease's dynamics. However, these models have not effectively considered the influence of double doses of vaccines, the incubation period, and vertical transmission of VZV during pregnancy simultaneously. In our study, we created a comprehensive delay mathematical model that incorporates the disease's incubation period, double-dose vaccination, and vertical transmission, as mentioned and cited in studies [1], [2], [10]. By using a delay differential equation, our model aims to offer valuable insights into the behavior and dynamics of chickenpox. To accurately capture the temporal aspects of the disease, we utilized a delay differential equation used in the studies [21], [22], [23], resulting in the development of an $SVPITR$ delay mathematical model. The rest part of this paper is structured as follows: Section 2 provides the model description and formulation, Section 3 covers model analysis and sensitivity analysis, Section 4 discusses the numerical simulation of the model, and Section 5 presents the study's discussion and conclusions.

2 Description, Assumptions and Formulation of the Model

To develop this model, we studied the biological behavior of chickenpox and its prevention mechanisms. We divided the entire population into six classes: susceptible($S(t)$), vaccinated($V(t)$), permanently immunized($P(t)$), infectious ($I(t)$), treated ($T(t)$), and recovered ($R(t)$) classes. The susceptible class increases based on recruitment rate of π and the attrition rates ω for the first vaccine dose. This class decreases based on contact rates β and when the first dose is administered by rate of α. The number of vaccinated individuals increases in α proportion to the susceptible class, and the proportions of recruits receiving the first vaccination dose by rate of η and decreases while receiving a double dose of vaccine causes a decrease in this class by rate of δ. Due to the waning effectiveness of the first vaccination dose by rate of ω, individuals in the vaccinated class will move to the susceptible group. The number of individuals in the infected class rapidly increases due to vertical transmission during pregnancy at a rate of θ, reactivation from the recovered class at a rate of σ, and the contact rate β. This class decreases due to the death rate from chickenpox at a rate of ϕ and the treatment rate γ. The recovery rate and treatment strategies cause the number of individuals in the recovered class to increase at a rate of ϑ and γ, respectively. The permanently immunized class increases with the double-dose vaccination rate δ and all classes decrease due to natural death rates μ.

The model was developed based on the following assumptions:

- The number of susceptible individuals increases due to immigrants and non-chickenpox-infected newborns.
- If a mother is infected during pregnancy, the newborn will inherit the virus from the mother.
- Chickenpox-infected individuals may die from the disease or develop temporary immunity.
- Individual in the recovered class may experience reactive symptoms several years later and revert to the infected class.
- A person who received only a single dose could be susceptible to the virus again.
- Everyone must receive double doses to be protected against the VZV virus for the rest of their lives.
- All the parameters that will be considered are positive.

We assumed that individuals exposed to VZV at a given time $t-\tau$ become infected at a later time τ and remain in the exposed class for a certain period until becoming infected. The number of individuals in the exposed class was assumed to be expressed as a bilinear incidence rate $\beta S(t-\tau)I(t-\tau)$. Not all people exposed to chickenpox survive for more than τ time units. For this reason, we can introduce the concept of lifetime (survival period), which is denoted by $e^{-\mu\tau}$. Therefore, the infectivity is expressed as $\beta(t-\tau)I(t-\tau)e^{-\mu\tau}$. This assumption is based on the ideas of many authors, such as [17], [21], [23]. Thus, from the description and assumption, the Figure 1 (Appendix) is constructed. From the schematic diagram, Figure 1 (Appendix), the following system

of delay differential equation is formulated:

$$\begin{cases} \frac{dS}{dt} = \pi + \omega V(t) - \beta S(t-\tau)I(t-\tau)e^{-\mu\tau} - (\alpha+\mu)S(t), \\ \frac{dV}{dt} = \eta + \alpha S(t) - (\mu+\delta+\omega)V(t), \\ \frac{dP}{dt} = \delta V(t) - \mu P(t), \\ \frac{dI}{dt} = \beta S(t-\tau)I(t-\tau)e^{-\mu\tau} + \delta R(t) - (\mu+\rho+\varphi-\theta)I(t), \\ \frac{dT}{dt} = \rho\gamma I(t) - (\mu+\vartheta+\epsilon)T(t), \\ \frac{dR}{dt} = (1-\rho)\gamma I(t) + \vartheta T(t) - (\mu+\delta)R(t). \end{cases} \quad (1)$$

with initial condition, $S_0 > 0$, $V_0 \geq 0$, $P_0 \geq 0$,$I_0 \geq 0$, $T_0 \geq 0$, and $R_0 \geq 0$, the parameters used in equation (1) are presented along with their descriptions in Table 1 (Appendix).

3 Model Analysis

This section describes the qualitative analysis of the model, including positivity, boundedness, equilibrium point, basic reproductive number, and sensitivity analysis.

3.1 Positivity and Boundedness of the Solutions

The state variables and corresponding parameters are assumed to be positive for biological reasons and represent the type and proportion of the population [24].

Theorem 1 *For all values of $t > 0$ with initial conditions $S(0) > 0$, $V(0) \geq 0$, $P(0) \geq 0$, $I(0) \geq 0$, $T(0) \geq 0$ and $R(0) \geq 0$, then all components of the solution i.e., $S(t), V(t), P(t), T(t), I(t)$, and $R(t)$ are non-negative.*

Proof. Let us prove this theorem by considering each equation in system of equation (1). To show that all $S(t), V(t), P(t), I(t)$, and $R(t)$ are non-negative, take the first equation of the system of equations (1).

$$\frac{dS}{dt} = \pi + \omega V(t) - \beta S(t-\tau)I(t-\tau)e^{(-\mu\tau)} - (\alpha + \mu)S(t). \quad (2)$$

This leads to,

$$\frac{dS}{dt} \geq -\left(\beta S(t-\tau)I(t-\tau)e^{-\mu\tau} + (\alpha+\mu)S(t)\right). \quad (3)$$

Since Equation (3) cannot be solved easily using the method of separation of variables, it is necessary to adopt assumptions previously employed by other researchers, such as those in [7]. According to the study reported in [23], $S(t-\tau)$ and $I(t-\tau)$denote the proportions of individuals who are released from susceptibility and those who are infected but not yet infectious, respectively.

$$\lim_{t\to\infty} S(t-\tau) = S \text{ and } \lim_{t\to\infty} I(t-\tau) = I.$$

As a result using the above assumption and separation of variable method on equation (3) we obtain:

$$S(t) = S(0)exp(-\int (\beta I e^{-\mu\tau} + \alpha + \mu)dt).$$

Similarly, the solution for other compartments would be: $V(t) \geq V(0)exp(-(\delta+\omega+\mu)t)$, $P(t) \geq P(0)exp(-\mu t)$, $I(t) \geq I(0)exp(-(\mu+\gamma+\phi-\theta)t)$, $T(t) \geq T(0)exp(-(\mu+\vartheta+\epsilon)t)$, and $R(t) \geq R(0)exp(-(\mu+\rho)t)$.

Here, the solutions for all compartments are given in exponential form. Since all non-negative initial values in each compartment are positive, then $S(t) > 0, V(t) > 0, P(t) > 0, I(t) > 0,$ and $R(t) > 0$. Boundedness reveals the regions in which solutions to a system of equations make biological and mathematical sense [25].

Theorem 2: *The feasible solution set $\{S, V, P, I, T, R\}$ of the model (1) with the given initial condition remains bounded in the region $\Omega = \left\{(S, V, P, I, T, R) \in \mathbb{R}_+^6 : 0 \leq N \leq \frac{\pi+\eta}{\mu}\right\}$.*

Proof. The total population at a given time t $N(t)$ is given by

$$N(t) = S(t) + V(t) + P(t) + I(t) + T(t) + R(t). \quad (4)$$

Differentiating N in equation (4) with respect to t we obtain

$$\frac{dN}{dt} = \frac{dS}{dt} + \frac{dV}{dt} + \frac{dP}{dt} + \frac{dI}{dt} + \frac{dT}{dt} + \frac{dR}{dt}. \quad (5)$$

Using system (1) and evaluating at (4) gives us;

$$\frac{dN}{dt} = \pi + \eta - (\phi+\theta)I(t) - \epsilon T(t) - \mu N(t).$$

Since the state variable of the system I and T are positive for all $t \geq 0$ we have

$$\frac{dN}{dt} \leq \pi + \eta - \mu N, \quad (6)$$

from which N is asymptotically bounded $i.e. 0 \leq N \leq \frac{\pi+\eta}{\mu}$. This completes the proof

3.2 Disease-free Equilibrium Point

We determine the equilibrium point at which the disease is eradicated from the population by letting the

right-hand side of equation (1) to zero and $I = T = R = 0$.

$$E_0 = (S_0, V_0, P_0, I_0, T_0, R_0) = \left(\frac{(\mu+\delta+\omega)\pi+\omega\eta}{(\alpha+\mu)(\mu+\delta)+\mu\omega}, \frac{\pi\alpha+\eta(\alpha+\mu)}{(\alpha+\mu)(\mu+\delta)+\mu\omega}, \frac{\pi\alpha\delta+\eta\mu(\alpha+\mu)}{\mu((\alpha+\mu)(\mu+\delta)+\mu\omega)}, 0,0,0\right) \quad (7)$$

3.3 Basic Reproductive Number

The basic reproductive number (R_0) is defined as how many people on average can be infected by an infected individual over the course of infectious period in a totally susceptible population. We will use the next generation matrix [7] to find the R_0 corresponding to the disease-free equilibrium given in equation (7). Let the matrix for new infection appearance at infected compartment be given by $\mathcal{F}$,

$$\mathcal{F} = \begin{bmatrix} I \\ T \end{bmatrix} = \begin{bmatrix} \beta S(t-\tau)I(t-\tau)e^{-\mu\tau} + \sigma R(t) + \theta I(t) \\ 0 \end{bmatrix}, \quad (8)$$

and the matrix of other transactions at each of the infected compartments be represented by $\mathcal{V}$, and is given by

$$\mathcal{V} = \begin{bmatrix} I \\ T \end{bmatrix} = \begin{bmatrix} (\mu+\gamma+\varphi)I(t) \\ -\rho\gamma I(t) + (\mu+\vartheta+\epsilon)T(t) \end{bmatrix}. \quad (9)$$

Now finding the Jacobian of $\mathcal{F}$ and $\mathcal{V}$ we get matrices F and V written as

$$F = \begin{bmatrix} \beta S(t-\tau)e^{-\mu\tau} + \theta & 0 \\ 0 & 0 \end{bmatrix}, \quad (10)$$

and

$$V = \begin{bmatrix} \mu+\gamma+\varphi & 0 \\ -\rho\gamma & \mu+\vartheta+\epsilon \end{bmatrix}. \quad (11)$$

Evaluating F at E_0 and finding V^{-1} we get,

$$F(E_0) = \begin{bmatrix} \beta e^{-\mu\tau}\left(\frac{(\mu+\delta+\omega)+\omega\eta}{(\alpha+\mu)(\mu+\delta)+\mu\omega}\right) + \theta & 0 \\ 0 & 0 \end{bmatrix}, \quad (12)$$

and

$$V^{-1} = \begin{bmatrix} \frac{1}{\mu+\gamma+\varphi} & 0 \\ \frac{\rho\gamma}{(\mu+\gamma+\varphi)(\mu+\vartheta+\epsilon)} & \frac{1}{\mu+\vartheta+\epsilon} \end{bmatrix}, \quad (13)$$

Then R_0 corresponding to E_0 is given by

$$R_0 = \nu(F(E_0) \times V^{-1}),$$

where, ν is the spectral radius of the matrix.

Therefore, the basic reproductive number with (R_0) and without delay $\left(R_0^d\right)$ can be explicitly written as

$$R_0 = \frac{((\mu+\delta+\omega)\pi+\omega\eta)\beta e^{-\mu\tau}}{((\alpha+\mu)(\mu+\delta)+\mu\omega)(\mu+\gamma+\varphi)} + \frac{\theta}{(\mu+\gamma+\varphi)}. \quad (14)$$

$$R_0^d = \frac{((\mu+\delta+\omega)\pi+\omega\eta)\beta}{((\alpha+\mu)(\mu+\delta)+\mu\omega)(\mu+\gamma+\varphi)} + \frac{\theta}{(\mu+\gamma+\varphi)}. \quad (15)$$

Remark: Since the survival term $e^{-\mu\tau}$ is less than one then the basic reproductive number with delay (R_0) is always less than the reproductive number without delay R_0^d.

3.4 Stability Analysis for disease-free Equilibrium

3.4.1 Local Stability Analysis for the Disease-Free Equilibrium

Theorem 3: *The disease-free equilibrium E_0 of the system (1) is locally asymptotically stable if $R_0 < 1$ and unstable if $R_0 > 1$.*

Proof. The Jacobian matrix of the system (1) is given by:

$$\begin{bmatrix} -A_1 & \omega & 0 & \beta S(t-\tau)e^{-\mu\tau} & 0 & 0 \\ \alpha & -(\delta+\omega+\mu) & 0 & 0 & 0 & 0 \\ 0 & \delta & -\mu & 0 & 0 & 0 \\ \beta I(t-\tau)e^{-\mu\tau} & 0 & 0 & A_2 & 0 & \delta \\ 0 & 0 & 0 & \rho\gamma & -(\mu+\vartheta+\epsilon) & 0 \\ 0 & 0 & 0 & (1-\rho)\gamma & \vartheta & -(\mu+\delta) \end{bmatrix} \quad (16)$$

where, $A_1 = \beta I(t-\tau)e^{-\mu\tau} + \alpha + \mu$ and $A_2 = \beta S(t-\tau)e^{-\mu\tau} - (\mu+\gamma+\vartheta-\theta)$. Evaluating the Jacobian matrix (16) at the disease free equilibrium E_0 we get:

$$J(E_0) = \begin{bmatrix} -X_1 & \omega & 0 & -X_6 & 0 & 0 \\ \alpha & -X_2 & 0 & 0 & 0 & 0 \\ 0 & \delta & -\mu & 0 & 0 & 0 \\ X_6 & 0 & 0 & X_3 & 0 & \delta \\ 0 & 0 & 0 & \rho\gamma & -X_4 & 0 \\ 0 & 0 & 0 & (1-\rho)\gamma & \vartheta & -k_5 \end{bmatrix}. \quad (17)$$

where, $X_1 = \alpha + \mu$, $X_2 = \delta + \omega + \mu$, $X_3 = \frac{\beta((\mu+\delta+\omega)\pi+\omega\eta)e^{-\mu\tau}}{(\alpha+\mu)(\mu+\delta)+\mu\omega} - (\mu+\gamma+\vartheta-\theta)$, $X_4 = \beta S(t-\tau)e^{-\mu\tau}$, $X_5 = \mu+\vartheta+\epsilon$ and $X_6 = \mu+\delta$. Whose characteristic polynomial is written as

$$P(\lambda) = (\mu+\lambda)(\lambda^2 + d_1\lambda + d_2)(\lambda^3 + d_3\lambda^2 + d_4\lambda + d_5) = 0, \quad (18)$$

where, $d_1 = X_1 + X_2$, $d_2 = X_1X_2 - \alpha\omega$, $d_3 = X_6 + X_5 - X_3$, $d_4 = X_6X_5 + \rho\delta\gamma - X_6X_3 - X_3X_5 - \delta\gamma$, and $d_5 = -X_6X_3X_5 + \delta\rho\gamma\vartheta - \gamma\delta(1-\rho)X_5$. From equation (18) we can get the characteristic root as

$$\mu + \lambda = 0 \Rightarrow \lambda = -\mu \quad (19)$$

or

$$\lambda^2 + d_1\lambda + d_2 = 0 \quad (20)$$

or

$$\lambda^3 + d_3\lambda^2 + d_4\lambda + d_5 = 0 \quad (21)$$

To get the root of both quadratic and cubic polynomial stated in equation (20) and (21) we used

the Routh-Hurwitz stability criterion [26]. For $\lambda^2 + d_1\lambda + d_2 = 0$ we have:

$$d_1 = X_1 + X_2 = \alpha + 2\mu + \delta + \omega > 0. \quad (22)$$

$$d_2 = X_1 * X_2 - \alpha\omega = (\alpha + \mu)(\delta + \mu) + \omega\mu > 0. \quad (23)$$

Since coefficients of the variable and constant term are greater than zero, equation (21) has strictly negative real root. For $\lambda^3 + d_3\lambda^2 + d_4\lambda + d_5 = 0$ we have,

$$d_3 = X_6 + X_5 - X_3 = (2\mu + \delta + \vartheta + \epsilon) - [(\mu + \gamma + \vartheta)(R_0 - 1)]. \quad (24)$$

$$d_4 = X_6X_5 + \rho\delta\gamma - X_6X_3 - X_3X_5 - \delta\gamma, = (\mu + \delta)(\mu + \vartheta + \epsilon) - (\mu + \gamma + \varphi)(R_0 - 1)(2\mu + \delta + \vartheta + \epsilon) + \delta\gamma(1 - \rho). \quad (25)$$

$$d_5 = -X_6X_3X_5 + \delta\rho\gamma\vartheta - \gamma\delta(1 - \rho)X_5, = -(\mu + \vartheta + \epsilon)[(\mu + \delta)(\mu + \gamma + \vartheta)(R_0 - 1) + \gamma\delta(\rho - 1)] + \delta\rho\gamma\theta. \quad (26)$$

$$d_3d_4 - d_5 = X_3^3(X_6 + X_5) - (\mu + \gamma + \vartheta)(R_0 - 1)\left(2X_6X_5 + X_5^2 + X_6^2 + \gamma\delta(1 - \rho)\right) + \delta\gamma(1 - \rho)X_6 + X_6X_5^2 + X_5X_6^2 + \sigma\rho\delta\vartheta. \quad (27)$$

When $R_0 < 1$, then $d_3 > 0, d_4 > 0, d_5 > 0$,and $d_3d_4 > d_5$. So equation (21) has strictly negative real root and E_0 is locally asymptotically stable and when $R_0 > 1$, at least one of the root of the characteristic equation (18) has a positive real root and E_0 is unstable. To investigate the global stability of disease-free equilibrium, we use the technique implemented in the study by [27]. Let's write the model system (1) as:

$$\frac{dU}{dt} = F(U, Z),$$
$$\frac{dZ}{dt} = G(U, Z),$$
$$G(U, 0) = 0,$$

where U represents an uninfected individual, i.e., $U = (S, V, P, R)^T \in \mathbb{R}_+^4$ and Z represents infected individuals, i.e, $Z = (I, T)^T \in \mathbb{R}_+^2$. Thus, the disease-free equilibrium point of the model can be represented by $E_0 = (U_0, 0)$. For $R_0 < 1$, for which the disease-free equilibrium point is locally asymptotically stable, the following two conditions are sufficient to guarantee the global stability of disease-free equilibrium point $(U_0, 0)$.

i. For $\frac{du}{dt} = F(U, 0)$, U_0 is globally asymptotically stable.
ii. $G(U, Z) = AZ - \tilde{G}(U, Z)$, where $\tilde{G}(U, Z) \geq 0$ for all $(U, Z) \in \Omega$

where $A = D_IG(U_0, 0)$ is a M-matrix (the off-diagonal elements of A are non-negative) and Ω is the region where the model makes biological sense.

3.4.2 Global Stability Analysis for the Disease-Free Equilibrium

Theorem 4: *The point $E_0 = (U_0, 0)$ is globally asymptotically stable provided that $R_0 < 1$ and the conditions expressed in (H1) and (H2) are satisfied.*

Proof. For condition (H1) from the system (1) we can get $F(U, Z)$

$$F(U, Z) = \begin{bmatrix} \pi + \omega V(t) - \beta S(t - \tau)I(t - \tau)e^{-\mu\tau} - (\alpha + \mu)S(t) \\ \eta + \alpha S(t) - (\mu + \delta + \omega)V(t) \\ \delta V(t) - \mu P(t) \\ (1 - \rho)\gamma I(t) + \vartheta T(t) - (\mu + \delta)R(t) \end{bmatrix} \quad (28)$$

Hence,

$$F(U, 0) = \begin{bmatrix} \pi + \omega V(t) - (\alpha + \mu)S(t) \\ \eta + \alpha S(t) - (\mu + \delta + \omega)V(t) \\ \delta V(t) - \mu P(t) \\ 0 \end{bmatrix}. \quad (29)$$

It is obvious that $U_0 = \left(\frac{(\mu+\delta+\omega)\pi+\omega\eta}{(\alpha+\mu)(\mu+\delta)+\mu\omega}, \frac{\pi\alpha+\eta(\alpha+\mu)}{(\alpha+\mu)(\mu+\delta)+\mu\omega}, \frac{\pi\alpha\delta+\eta\mu(\alpha+\mu)}{\mu((\alpha+\mu)(\mu+\delta)+\mu\omega)}, 0\right)$ is globally asymptotically stable for $F(U, 0)$ as $U \to U_0$ when $t \to \infty$. For condition (H2), from the system (1) we can get $G(U, Z)$ as follow:

$$G(U, Z) = \begin{bmatrix} \beta S(t - \tau)I(t - \tau)e^{-\mu\tau} + \delta R(t) - (\mu + \rho + \varphi - \theta)I(t) \\ \rho\gamma I(t) - (\mu + \vartheta + \epsilon)T(t) \end{bmatrix}, \quad (30)$$

and

$$A = \begin{bmatrix} \beta S(t - \tau)e^{-\mu\tau} - (\mu + \rho + \varphi - \theta) & 0 \\ \rho\gamma & -(\mu + \vartheta + \epsilon) \end{bmatrix}. \quad (31)$$

We have,

$$\tilde{G}(U, Z) = AZ - G(U, Z). \quad (32)$$

$$= \begin{bmatrix} \tilde{G}_1(U, Z) \\ \tilde{G}_2(U, Z) \end{bmatrix} = \begin{bmatrix} -\delta R(t) \\ 0 \end{bmatrix}, \quad (33)$$

According to the approach outlined in study [28], equation (33) yields $\tilde{G}_1(U, Z) < 0$, which in turn implies $\tilde{G}_1(U, Z) < 0$. This indicates that the second condition (H2) is not fulfilled. Consequently, the disease-free equilibrium may fail to be globally asymptotically stable even when $R_0 < 1$.

3.5 Endemic Equilibrium Point

The endemic equilibrium point E^* occurs when the chickenpox disease persist in the community. We

determine it by letting the right hand side of equation (1) to zero

$$E^* = \Bigg\{(S^*, V^*, P^*, I^*, T^*, R^*) = \frac{\left((\mu+\vartheta+\epsilon)\left((\mu+\varphi-\theta)(\mu+\delta)+\gamma\mu\right)+\rho\delta\gamma(\mu+\epsilon)\right)e^{\mu\tau}}{(\mu+\vartheta+\epsilon)(\mu+\delta)\beta}, \frac{\alpha\delta}{(\mu+\delta+\omega)\mu}\left(\frac{\eta}{\alpha}+S^*\right), \frac{\mu}{\delta}P^*, \frac{e^{\mu\tau}(\pi+\omega V^*-(\alpha+\mu)S^*)}{\beta S^*}, \frac{\rho\gamma}{(\mu+\vartheta+\epsilon)}I^*, \frac{(1-\rho)\gamma I^*+\vartheta T^*}{(\mu+\delta)}\Bigg\}. \quad (34)$$

3.6 Stability Analysis for Endemic Equilibrium

3.6.1 Local Stability of the Endemic Equilibrium

Theorem 5: *An endemic equilibrium of system of equation (1) is locally asymptotically stable when* $R_0 > 1$, *and unstable otherwise.*

Proof. At the endemic equilibrium point, the Jacobian matrix J of the system of equations (1) is derived as follows:

$$J(E^*) = \begin{bmatrix} -k_1 & \omega & 0 & -k_6 & 0 & 0 \\ \alpha & -k_2 & 0 & 0 & 0 & 0 \\ 0 & \delta & -\mu & 0 & 0 & 0 \\ k_6 & 0 & 0 & k_3 & 0 & \delta \\ 0 & 0 & 0 & \rho\gamma & -k_4 & 0 \\ 0 & 0 & 0 & (1-\rho)\gamma & \vartheta & -k_5 \end{bmatrix}, \quad (35)$$

where, $k_1 = (\beta I^* e^{-\mu\tau} + \alpha + \mu)$, $k_2 = (\delta + \omega + \mu)$, $k_3 = \beta S^* e^{-\mu\tau} - (\mu + \gamma + \varphi - \theta)$, $k_4 = (\mu + \vartheta + \epsilon)$, $k_5 = (\mu + \delta)$, $k_6 = \beta S^* e^{-\mu\tau}$. Whose characteristic polynomial is written as

$$P(\lambda) = -(\mu + \lambda)(\lambda^5 + y_1\lambda^4 + y_2\lambda^3 + y_3\lambda^2 + y_4\lambda + y_5). \quad (36)$$

where, $y_1 = c - a$, $y_2 = d + ac + m - b$, $y_3 = da + cb + h + fm$, $y_4 = ea + bd + fh + gm + e$, $y_5 = eb + gh$ and $a = k_5 + k_4, b = k_5k_4, c = k_3 - k_1 - k_2, d = k_1k_3 - k_6^2 + k_2(k_3 - k_1) + \omega\alpha, e = k_1k_2k_3 - k_2k_6^2 - k_3\omega\alpha, f = k_2 + k_1, g = k_1k_2, h = ((1-\rho)k_4 + \rho\vartheta)\gamma\delta, m = (1-\rho)\gamma\delta$. If $R_0 > 1$, then the following conditions are satisfied: $y_1 > 0$, $y_2 > 0$, $y_3 > 0$, $y_4 > 0$, $y_5 > 0$, $y_1y_2 - y_3 > 0$, $y_1y_2y_3 - y_1^2y_4 - y_3^2 > 0$ and $y_5^2y_3y_1 - y_5^3 - y_5^2y_2^2y_1 - y_5^2y_3^2y_2^2 + y_5^2y_4y_1 - y_1^2y_4^2y_5 - y_1y_2y_3y_4y_5 - y_4y_5y_3^2 > 0$. Therefore, by the Routh-Hurwitz criterion, the endemic equilibrium is locally asymptotically stable if $R_0 > 1$.

3.6.1 Global Stability of the Endemic Equilibrium

Theorem 6: *endemic equilibrium of the model (1) is globally asymptotically stable if* $R_0 > 1$.

Proof. Following the approach in [27] and constructing a Lyapunov function as introduced in [29], we construct the subsequent equation in order to rigorously verify the theorem:

$$\mathcal{G}(t) = \left(S - S^* - ln\left(\frac{S^*}{S}\right)\right) + \left(V - V^* - ln\left(\frac{V^*}{V}\right)\right) + \left(P - P^* - ln\left(\frac{P^*}{P}\right)\right) + \left(I - I^* - ln\left(\frac{I^*}{I}\right)\right) + \left(T - T^* - ln\left(\frac{T^*}{T}\right)\right) + \left(R - R^* - ln\left(\frac{R^*}{R}\right)\right). \quad (37)$$

Differentiating equation (37) with respect to t we get

$$\frac{d\mathcal{G}}{dt} = \left(1 - \frac{S^*}{S}\right)\frac{dS}{dt} + \left(1 - \frac{V^*}{V}\right)\frac{dV}{dt} + \left(1 - \frac{P^*}{P}\right)\frac{dP}{dt} + \left(1 - \frac{I^*}{I}\right)\frac{dI}{dt} + \left(1 - \frac{T^*}{T}\right)\frac{dT}{dt} + \left(1 - \frac{R^*}{R}\right)\frac{dR}{dt}.$$

Substituting $\frac{dS}{dt}, \frac{dV}{dt}, \frac{dP}{dt}, \frac{dI}{dt}, \frac{dT}{dt}, \frac{dR}{dt}$ from (1) to equation (38) and after some rearrangement, we get

$$\frac{d\mathcal{G}}{dt} = \pi + \beta IS^*e^{-\mu\tau} + (\alpha + \mu)S^* + \eta + (\mu + \delta + \omega)V^* + \mu P^* + (\mu + \gamma + \varphi)I^* + (\mu + \vartheta + \epsilon)T^* + (\mu + \sigma)R^* + \theta I + \rho\gamma I\frac{R^*}{R} - \left(\mu S + (\pi + \omega V)\frac{S^*}{S} + \mu V + (\eta + \alpha S)\frac{V^*}{V} + \mu P + \delta V\frac{P^*}{P} + (\mu + \varphi)I + \beta SI^*e^{-\mu\tau} + \delta R\frac{I^*}{I} + \theta I^* + \rho\gamma\ I\frac{T^*}{T} + \mu R + (\gamma I + \vartheta T)\frac{R^*}{R}\right). \quad (39)$$

For equation (40), if we represent the positive part by Q_1 and the negative part by Q_2, then equation (39) can be simplified as follows.

$$\frac{d\mathcal{G}}{dt} = Q_1 - Q_2. \quad (40)$$

Thus, if $Q_1 < Q_2$, then $\frac{d\mathcal{G}}{dt} \leq 0$ and $\frac{d\mathcal{G}}{dt} = 0$ if and only if $S = S^*$, $V = V^*$, $P = P^*$, $I = I^*$,$T = T^*$and $R = R^*$. Therefore, the largest compact invariant set in $\left\{(S^*, V^*, P^*, I^*, T^*, R^*) \in \Omega: \frac{d\mathcal{G}}{dt} = 0\right\}$ is the singleton E^*. By LaSalle's invariant principle [30], it implies that E^* is globally asymptotically stable in Ω if $Q_1 < Q_2$.

3.7 Sensitivity Analysis

Here we explained the sensitivity analysis of the developed model. This will help to determine the influence of basic parameters on the dynamics of chickenpox. The sensitivity index with respect to a parameter h_i is given by a normalized sensitivity index [30],

$$H_{h_i}R_0 = \frac{\partial R_0}{\partial h_i} \times \frac{h_i}{R_0},$$

where, h_i represent all the basic parameters. Hence,

$H_\beta R_0 = \frac{\partial R_0}{\partial \beta} \times \frac{\beta}{R_0} = \frac{((\mu+\delta+\omega)\pi+\omega\eta)\beta e^{-\mu\tau}}{((\mu+\delta+\omega)\pi+\omega\eta)\beta e^{-\mu\tau}+((\alpha+\mu)(\mu+\delta)+\mu\omega)\theta},$

$H_\alpha R_0 = \frac{\partial R_0}{\partial \alpha} \times \frac{\alpha}{R_0} = -\frac{\beta\alpha(\mu+\delta)((\mu+\delta+\omega)\pi+\omega\eta)}{(((\mu+\delta+\omega)\pi+\omega\eta)\beta+((\alpha+\mu)(\mu+\delta)+\mu\omega)\theta e^{\mu\tau})((\alpha+\mu)(\mu+\delta)+\mu\omega)},$

$H_\omega R_0 = \frac{\partial R_0}{\partial \omega} \times \frac{\omega}{R_0} = \frac{\beta\omega(\mu+\delta)(\alpha(\pi+\eta)+\eta)}{(((\mu+\delta+\omega)\pi+\omega\eta)\beta+((\alpha+\mu)(\mu+\delta)+\mu\omega)\theta e^{\mu\tau})((\alpha+\mu)(\mu+\delta)+\mu\omega)},$

$H_\delta R_0 = \frac{\partial R_0}{\partial \delta} \times \frac{\delta}{R_0} = -\frac{\mu\omega\eta\delta\beta}{(((\mu+\delta+\omega)\pi+\omega\eta)\beta+((\alpha+\mu)(\mu+\delta)+\mu\omega)\theta e^{\mu\tau})((\alpha+\mu)(\mu+\delta)+\mu\omega)},$

$H_\gamma R_0 = \frac{\partial R_0}{\partial \gamma} \times \frac{\gamma}{R_0} = -\frac{\gamma(((\mu+\delta+\omega)\pi+\omega\eta)\beta e^{-\mu\tau}+\theta(\mu+\delta+\vartheta)^2)}{((\mu+\gamma+\vartheta))((\mu+\delta+\omega)\pi+\omega\eta)\beta e^{-\mu\tau}+((\alpha+\mu)(\mu+\delta)+\mu\omega)\theta} < 0,$

$H_\theta R_0 = \frac{\partial R_0}{\partial \theta} \times \frac{\theta}{R_0} = \frac{\theta((\alpha+\mu)(\mu+\delta)+\mu\omega)}{((\mu+\delta+\omega)\pi+\omega\eta)\beta e^{-\mu\tau}+((\alpha+\mu)(\mu+\delta)+\mu\omega)\theta} > 0,$

$H_\tau R_0 = \frac{\partial R_0}{\partial \tau} \times \frac{\tau}{R_0} = \frac{\tau\mu((\mu+\delta+\omega)\pi+\omega\eta)\beta e^{-\mu\tau}}{(((\mu+\delta+\omega)\pi+\omega\eta)\beta e^{-\mu\tau}+((\alpha+\mu)(\mu+\delta)+\mu\omega)\theta)((\alpha+\mu)(\mu+\delta)+\mu\omega)(\mu+\gamma+\vartheta)}$

.

The sensitivity analysis presented in Table 2 (Appendix) and Figure 2 (Appendix) shows that the R_0increases with parameters that have positive sensitivity indices, including the contact rate (β), the loss rate of the first vaccination (ω), and the vertical transmission rate (θ), while other parameters remain unchanged. This highlights the strong influence of these parameters on increasing the average number of individuals infected with chickenpox. In contrast, parameters with negative sensitivity indices contribute to a reduction in disease transmission. In particular, increasing the incubation period (τ), recovery rate (γ), first vaccination rate $(\alpha$, and second vaccination rate (δ) leads to a decrease in R_0 derived from the model. These results indicate that enhanced vaccination coverage and faster recovery dynamics play a crucial role in limiting the spread of the disease.

Generally, the sensitivity analysis gives strong epidemiological insights as well as practical disease control recommendations. Interventions that improve factors with negative sensitivity indices, such as vaccination and recovery rates, while decreasing the value of parameters with positive sensitivity indices, such as contact and transmission rates, are likely to be effective in reducing the spread of chickenpox. Consequently, prioritizing immunization programs and targeted preventative efforts based on these findings can significantly lower the illness burden in the community.

4 Numerical Simulation and Discussion

In our study, we rigorously verified the model's reliability by conducting numerical simulations using the parameter values provided in Table 3 (Appendix). To graphically display the model, we have used the MATLAB 2019a computer software. The importance of graphically exhibiting the model helps us for more effective visualization and interpretation of the outcomes. This visual representation of the model in numerical simulations investigated the dynamics of infected classes, taking into account aspects such as delay with saturation incidence, double vaccination doses, and vertical transmission. We keenly observed how the system responded over time to changes in fundamental parameters. As indicated in the introduction [2], chickenpox symptoms typically emerge every 10 to 21 days on average. By incorporating the incubation period in our model, we were able to retain exposed individuals in the analysis, enabling us to devise strategic control measures to curb the spread of chickenpox. Our analysis of the time delay in the model zeroed in on the maximum incubation period $(\tau = 21)$ as depicted in Figure 3 (Appendix). The investigation of the infected class in this figure revealed a consistent decrease in the number of infected individuals over the time delay (incubation period), signifying that individuals remained in the exposed class for a period before becoming infectious again. This underscores the significance of incorporating time delay into the mathematical model of chickenpox and other infectious diseases in retaining exposed individuals in the exposed class. Furthermore, it showcased a notable increase in the number of vaccinated, permanently immunized, recovered, and treated individuals during this period.

4.1 Effects of Contact Rate on Chickenpox-Infected Populations

Figure 4 (Appendix) illustrates the effect of varying the contact rate on the proportion of individuals infected with chickenpox. The numerical simulations show that increasing the contact rate significantly amplifies disease transmission, as susceptible individuals are more likely to acquire infection

through contact with infected individuals or virus-contaminated materials. This trend is particularly pronounced in populations where pregnant women are exposed to the virus, as maternal infection may result in vertical transmission to unborn children, thereby increasing the overall number of infected individuals. Additionally, newborns infected through vertical transmission and subsequently introduced into the community further contribute to sustained disease spread. To ensure the robustness of the numerical results, simulations were conducted by varying the contact rate parameter β within the range $\beta = 0.330$ to $\beta = 0.805$ while keeping all other parameters fixed. A scale refinement test was conducted to assess numerical stability. The solution trajectories revealed low divergence with moderate perturbations of β, indicating the numerical approach is stable. The presented trends are not the result of a discretization error. To promote interpretability, Figure 4 (Appendix) axes are clearly labeled with appropriate variable names and units.

4.2 Effects of Vertical Transmission Rate on Chickenpox-Infected Populations

The impact of vertical transmission on chickenpox dynamics is presented in Figure 5 (Appendix), motivated by epidemiological evidence reported in [1]. Numerical simulations were performed by varying the vertical transmission rate θ from 0.35 to 0.50. The results demonstrate that higher rates of maternal‑to‑fetal transmission substantially increase the number of infected individuals in the population. To assess numerical robustness, sensitivity analysis were performed by adding small perturbations to θ. The solution curves were qualitatively consistent. This demonstrates the scheme's numerical stability and supports the validity of the observed trends. These results emphasize the importance of preventing maternal infection to control congenital and community-level transmission of chickenpox.

4.3 Effect of First and Second Vaccination Rates on Chickenpox-Infected Population

This subsection explores the effect of the World Health Organization's recommended first and second vaccination rates on chickenpox transmission, while all other factors remain constant. As seen in Figure 6 (Appendix), increasing vaccination coverage significantly reduces the number of affected people. The result of this simulation indicate that the higher rates of first and second doses, reduce disease prevalence over time and can push the infection to eradication. To assess the robustness of these findings, vaccination parameters were adjusted within biologically realistic ranges, and numerical solutions were compared across this simulation. The generated trajectories showed some numerical error while maintaining consistent qualitative behavior, proving the numerical scheme's stability under parameter uncertainty. The data indicate the higher efficiency of double-dose MMRV immunization in decreasing infection.

4.4 Effect of Treatment and Recovery Rates on Chickenpox-Infected Population

Effective treatment and prompt recovery are critical to decreasing chickenpox transmission. Individuals who become infected should follow medical advice, which includes getting enough rest, staying hydrated, and receiving proper clinical care. Figure 7 (Appendix) depicts the effect of increased treatment and recovery rates on the number of affected individuals. The simulations indicate that higher recovery rates shorten the infectious period, thereby reducing secondary transmission. To assess numerical stability, simulations were performed using different step sizes and slight perturbations of recovery parameters. The resulting numerical solutions converged consistently, indicating low truncation error and strong stability of the computational method. These findings confirm that improvements in treatment and recovery rates significantly reduce disease burden and that the numerical results are robust with respect to parameter uncertainty.

5 Discussion and Conclusion

This study presents a comprehensive analysis of chickenpox transmission dynamics using a delayed $SVPITR$ mathematical model formulated as a system of delay differential equations. The proposed model explicitly incorporates key epidemiological features, including the incubation period, vertical transmission, and administration of the first and second doses of the $MMRV$ vaccine, consistent with existing modeling studies [1], [2], [24]. Using the next-generation matrix approach, the basic reproductive numbers for the models without and with time delay were computed as $R_0 = 2.3234$ and $R_0^d = 2.4742$, respectively, based on the parameter values reported in Table 3 (Appendix). These results validate the analytical

findings established in Section 3 and confirm that the endemic equilibrium is globally asymptotically stable whenever $R_0 > 1$.

The qualitative and analytical analyses show the epidemiological significance of employing time delay to portray the chickenpox incubation period. For example, delay affects the timing and magnitude of secondary infections, providing a more realistic picture of illness development. Numerical simulations reveal that reducing vertical transmission, increasing vaccine coverage, extending the incubation period, and enhancing recovery rates are all effective methods of reducing chickenpox transmission. These findings emphasize the importance of early infection prevention and immunization in preventing disease spread. The graphical representations developed with MATLAB 2019a provide visual support for these findings and reinforce the analytical conclusions. In contrast to prior research [2], [5], [10], [11], which mostly focused on preventative mechanisms and general control methods, the current study contributes to the literature by integrating vertical transmission, immunization with double-dose MMRV, and an explicit incubation delay. This integrated modeling methodology provides additional insight into disease transmission behavior and enables for a more thorough evaluation of therapeutic measures. As a result, the model advances our understanding of how vaccination, incubation delay, and vertical transmission affect chickenpox dynamics.

Despite these advances, various limitations of the constructed delayed $SVPITR$ model are discussed. First, the assumption of homogeneous mixing implies that individuals have equal contact probabilities. But, in reality contact patterns vary with different factors like age, social behavior, and spatial structure, potentially influencing disease transmission. The other limitation of this paper is the usage of parameter values we used for numerical simulations were obtained from existing literature or extrapolated from limited data sources. Uncertainty in these estimates, particularly those relating to contact rates, vaccination coverage, and vertical transmission, may affect the quantitative accuracy of model projections. Again also demographic variables such as population growth, migration, and seasonal change were not explicitly considered. Furthermore, while the constant time delay reflects the average incubation length, it does not account for individual diversity in incubation times. Incorporating dispersed delays or stochastic effects may result in a more realistic picture of illness development. The model also ignores potential decreasing immunity after the initial vaccine dosage, as well as behavioral changes caused by public health actions during epidemics. These restrictions imply that the suggested model should be viewed as a deterministic approximation of chickenpox transmission dynamics.

Nonetheless, the established framework establishes a solid analytical platform for future research. Potential enhancements include incorporating age structure, regional heterogeneity, stochastic dynamics, diminishing immunity, and data-driven parameter calibration. Such improvements would increase the model's relevance in informing public health policies and vaccination efforts targeted at the successful control and eventual eradication of chickenpox.

Declaration of Generative AI and AI-assisted Technologies in the Writing Process

During the preparation of this work, the author(s) utilized artificial intelligence (AI) technologies solely for the purpose of linguistic refinement and grammatical correction. Following the application of these tools, the author(s) comprehensively reviewed, verified, and edited the resulting text. The author(s) maintain full accountability and responsibility for the accuracy, integrity, and final content of the publication.

References:

[1] Zhang, X. S., Smith, A., Patel, B., Anderson, C., Pomeroy, L., Higgins, G., O'Moore, E., Chow, Y., & Atchison, C. (2020). New approaches to controlling an outbreak of chickenpox in a large immigration detention setting in England: The role of serological testing and mathematical modelling. Epidemiology and Infection, 148, e25. https://doi.org/10.1017/S095026882000014X.

[2] Agbata, B. C., Omale, D., Ojih, P. B., & Omatola, I. U. (2019). Mathematical analysis of chickenpox transmission dynamics with control measures. Dio, 10, 6–23.

[3] Almuallem, N. A., Ali, H. M., Elsaid, E. M., Eid, M. R., & Hassanin, W. S. (2024). Mathematical simulation of optimal control measures to avoid chickenpox infection. International Journal of Mathematics and Mathematical Sciences, 2025(1), 3238188. https://doi.org/10.1155/ijmm/3238188.

[4] Baker, R. E., Mahmud, A. S., & Metcalf, C. J.

E. (2018). Dynamic response of airborne infections to climate change: Predictions for varicella. Climatic Change, 148(4), 547–560. https://doi.org/10.1007/s10584-018-2204-44.

[5] Edward, S., Kuznetsov, D., & Mirau, S. (2014). Modeling and stability analysis for a varicella zoster virus model with vaccination. Applied and Computational Mathematics, 3(4), 150–162. https://doi.org/10.11648/j.acm.20140304.16.

[6] Madaki, Y. U., Manu, H. A., Gwani, A. A., & Edeghagba, E. E. (2020). Application of mathematical modelling on the spread of chicken pox disease (A case study of Naiyawna Clinic Damaturu, Yobe State). Scholars Journal of Physics, Mathematics and Statistics, 7, 260–271. https://doi.org/10.36347/sjpm.2020.v07i10.004.

[7] Nonthakorn, O. (2016). Biological models with time delay (Doctoral dissertation, Worcester Polytechnic Institute). Worcester Polytechnic Institute Digital WPI, [Online]. https://digital.wpi.edu/concern/student_works/08612q29z (Accessed Date: January 15, 2026).

[8] Singh, H. K., & Pandey, D. N. (2024). Analysis of the chickenpox disease evolution in an MSEIR model using fractal-fractional differential operator. Differential Equations and Dynamical Systems, 1–21. https://doi.org/10.1007/s12591-024-00690-1.

[9] Suzuki, A., & Nishihara, H. (2023). Seasonal transmission dynamics of varicella in Japan: The role of temperature and school holidays. Mathematical Biosciences and Engineering, 20(2), 4069–4081. https://doi.org/10.3934/mbe.2023190.

[10] Karsai, J., Csuma-Kovacs, R., Danielisz, A., et al. (2020). Modeling the transmission dynamics of varicella in Hungary. Journal of Mathematics in Industry, 10, 12. https://doi.org/10.1186/s13362-020-00079-z.

[11] Elisha, A., Aboiyar, T., & Kimbir, A. R. (2021). Mathematical analysis of varicella zoster virus model. International Journal of Discrete Mathematics, 6(2), 23–37.

[12] Biggerstaff, M., Slayton, R. B., Johansson, M. A., & Butler, J. C. (2021). Improving pandemic response: Employing mathematical modeling to confront COVID-19. Clinical Infectious Diseases, ciab673. https://doi.org/10.1093/cid/ciab673.

[13] Rao, D., Tanveer, A., Iftekhar, E. N., Müller, S. A., Sherratt, K., Röbl, K., Carrillo-Bustamante, P., Heldt, K., Fitzner, J., Hanefeld, J., & Funk, S. (2025). The utility of infectious disease modelling in informing decisions for outbreak response: A scoping review. PLOS Global Public Health, 5(9), e0005120. https://doi.org/10.1371/journal.pgph.0005120.

[14] Oliwa, J., Guleid, F. H., Owek, C. J., Maluni, J., Jepkosgei, J., Nzinga, J., Were, V. O., Sim, S. Y., Walekhwa, A. W., Clapham, H., & Dabak, S. (2025). Framework to guide the use of mathematical modelling in evidence-based policy decision-making. BMJ Open, 15(4), e093645. https://doi.org/10.1136/bmjopen-2024-093645.

[15] Kiselev, I. N., Akberdin, I. R., & Kolpakov, F. A. (2023). Delay-differential SEIR modeling for improved modelling of infection dynamics. Scientific Reports, 13, 13439. https://doi.org/10.1038/s41598-023-40008-9.

[16] Rihan, F. A. (2021). Delay differential equations with infectious diseases. In Delay Differential Equations and Applications to Biology (pp. 145–165). Springer. https://doi.org/10.1007/978-981-16-0626-7_8.

[17] Cooke, K. L., & van den Driessche, P. (1996). Analysis of an SEIRS epidemic model with two delays. Journal of Mathematical Biology, 35(2), 240–260. https://doi.org/10.1007/s002850050051.

[18] Alves, H., Oliveira, A., Silva, B., Morais, T., Dias, M. F., & Robaina, M. (2024). Analysing residential water demand in Portuguese municipalities and its implications in policymaking. WSEAS Transactions on Environment and Development, 20, 1148–1175. https://doi.org/10.37394/232015.2024.20.105.

[19] Kotola, B. S. (2024). A mathematical model for varicella-zoster and HIV co-dynamic supported by numerical simulations. PLOS ONE, 19(3), e0299734. https://doi.org/10.1371/journal.pone.0299734.

[20] Hariharan, S., Shangarganesh, L., Debbouche, A., et al. (2023). Stability analysis of spatiotemporal reaction-diffusion mathematical model incorporating the varicella virus transmission. European Physical Journal Plus, 138, 1123. https://doi.org/10.1140/epjp/s13360-023-04777-6.

[21] Kisiolek, A., Kubiaczyk, I., & Sikorska-Nowak,

A. (2019). Stability for functional differential equations with delay in Banach spaces. Advances in Pure Mathematics, 9, 337–346. https://doi.org/10.4236/apm.2019.94016.

[22] Kumar, A., & Nilam. (2019). Mathematical analysis of a delayed epidemic model with nonlinear incidence and treatment rates. Journal of Engineering Mathematics, 115(1), 1–20. https://doi.org/10.1007/s10665-019-09989-3.

[23] Naresh, R., Tripathi, A., Tchuencher, J. M., & Sharma, D. (2009). Stability analysis of a time delayed SIR epidemic model with nonlinear incidence rate. Computers & Mathematics with Applications, 58(2), 348–359. https://doi.org/10.1016/j.camwa.2009.03.110.

[24] Kudlus, M. A., Mohiuddin, M., & Rahman, A. (2021). Mathematical analysis of a measles transmission dynamics model in Bangladesh with double dose vaccination. Scientific Reports, 11(1), 16571. https://doi.org/10.1038/s41598-021-95913-8.

[25] Ogundare, B. S., & Akingbade, J. (2021). Boundedness and stability properties of solutions of mathematical model of measles. Tamkang Journal of Mathematics, 52(1), 91–112. https://doi.org/10.5556/j.tkjm.52.2021.3411.

[26] Mahardika, R., Widowati, & Sumanto, Y. D. (2019). Routh-Hurwitz criterion and bifurcation method for stability analysis of tuberculosis transmission model. Journal of Physics: Conference Series, 1217(1), 012056. https://doi.org/10.1088/1742-6596/1217/1/012056.

[27] Castillo-Chavez, C., Feng, Z., & Huang, W. (2002). On the computation of R_0 and its role on global stability. In Mathematical Approaches for Emerging and Reemerging Infectious Diseases: An Introduction (Vol. 125, pp. 229–250). Springer. https://doi.org/10.1007/978-1-4757-3667-0_13.

[28] Bello, K., Akinwande, I., Abdurhman, S., Kuta, A., & Bello, Y. (2019). Global stability analysis of the disease-free equilibrium state of a mathematical model of trypanosomiasis. Journal of Applied Sciences and Environmental Management, 23(2), 201–208. https://doi.org/10.4314/jasem.v23i2.1.

[29] LaSalle, J. P. (1976). The stability of dynamical systems. Society for Industrial and Applied Mathematics. https://doi.org/10.1137/1.9781611970432.

[30] Chitnis, N., Hyman, J. M., & Cushing, J. M. (2008). Determining important parameters in the spread of malaria through the sensitivity analysis of a mathematical model. Bulletin of Mathematical Biology, 70(5), 1272–1296. https://doi.org/10.1007/s11538-008-9299-0.

[31] Ogumiloro, O. (2020). On the asymptotic behavior and approximate solutions of varicella zoster virus model using modified differential transform method. https://doi.org/10.22541/au.159972851.10863161.

Contribution of Individual Authors to the Creation of a Scientific Article (Ghostwriting Policy)

All authors have equal contribution for this paper. All authors read and approved the manuscript.

Sources of Funding for Research Presented in a Scientific Article or Scientific Article Itself

No funding was received for conducting this study.

Availability of data and material:

The data we used for this paper is from the respective published articles that are cited.

Conflict of Interest

The authors declare that there is no conflict of interest regarding the publication of this paper.

Creative Commons Attribution License 4.0 (Attribution 4.0 International, CC BY 4.0)

This article is published under the terms of the Creative Commons Attribution License 4.0
https://creativecommons.org/licenses/by/4.0/deed.en_US

APPENDIX

Table 1. Parameters and their description

Parameters	Description
$\boldsymbol{\pi}$	Recruitment rate
$\boldsymbol{\beta}$	Rate of Contact
$\boldsymbol{\alpha}$	First vaccination rate
$\boldsymbol{\delta}$	Second vaccination dose rate
$\boldsymbol{\omega}$	Loss of first vaccination rate
$\boldsymbol{\eta}$	Vaccinated immigrant rate
$\boldsymbol{\mu}$	Natural death rate
$\boldsymbol{\epsilon}$	Rate of death due to disease in the treatment class
$\boldsymbol{\varphi}$	Rate of death due to the disease in the infected class
$\boldsymbol{\tau}$	Incubation period,
$\boldsymbol{\gamma}$	Infectious rate
$\boldsymbol{\theta}$	Rate of vertical transmission
$\boldsymbol{\vartheta}$	Progression rate
$\boldsymbol{\sigma}$	Rate of loss of temporary immunity
$\boldsymbol{\rho}$	Fraction of infected population

Source: created by the authors

Table 2. Sensitivity index table

Parameter	Sensitivity Indices
θ	0.9636
β	0.9343
ω	0.0057
α	-0.0058
δ	-0.0036
τ	-0.9162
γ	-0.9333

Source: created by the authors

Table 3. Parameter's value and their source

Parameter	Value	Reference
τ	21 days	[2]
ϑ	0.6 per day	[5]
γ	0.01923 per day	[10]
β	0.1431 per day	[10]
α	0.0052 per day	[31]
π	0.03876 per day	[31]
ω	0.00033 per day	[31]
δ	0.00002 per day	[31]
μ	0.3 per day	Assumed
θ	0.0241 per day	Assumed
ρ	0.125	Assumed
δ	0.2 per day	Assumed
φ	0.245 per day	Assumed
ϵ	0.1 per day	Assumed
η	0.265 per day	Assumed

Source: created by the authors

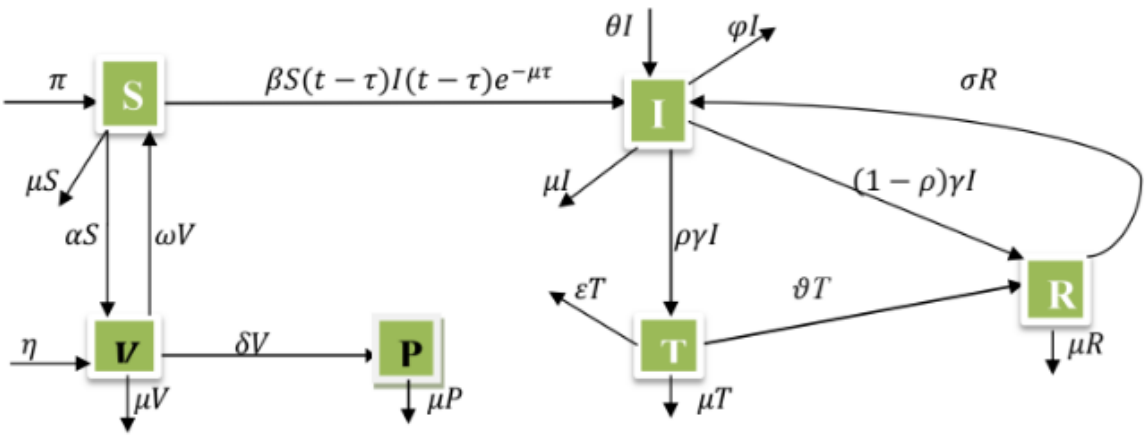


Fig. 1: Disease transmission diagram

Source: created by the authors

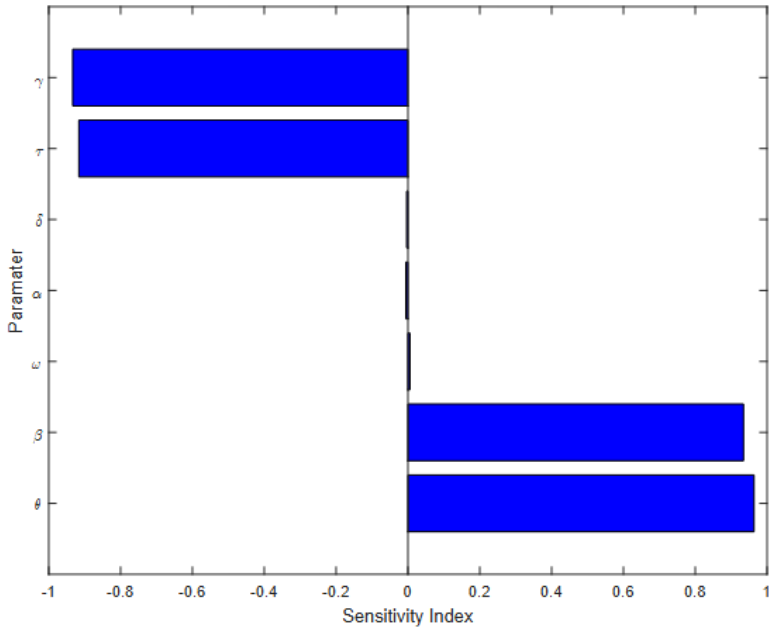


Fig. 2: Sensitivity indices of the R_0
Source: created by the authors

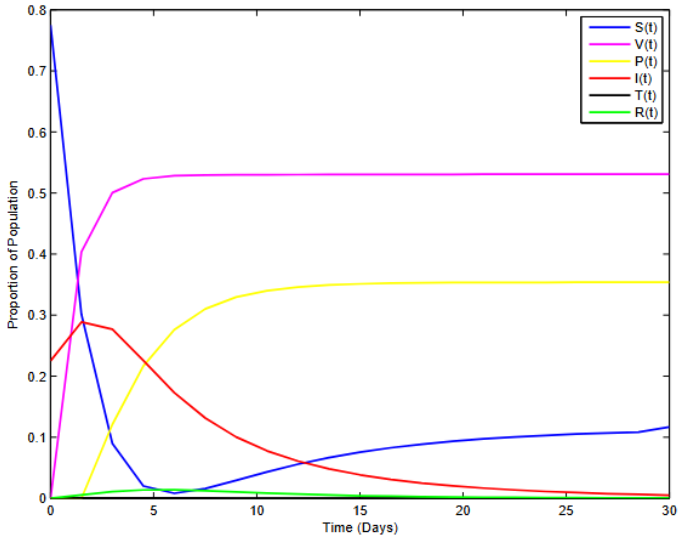


Fig. 3: Graph of a system of delay differential equations (1) with all parameters
Source: created by the authors

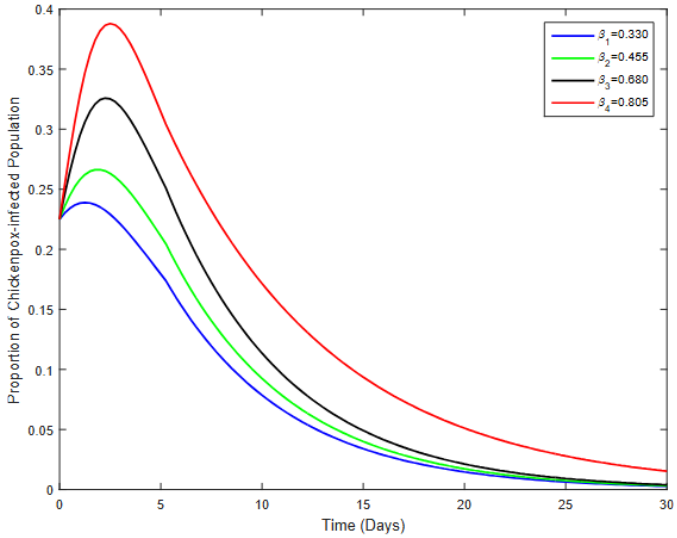


Fig. 4: Effect of contact rate β on the proportion of chickenpox‑infected individuals
Source: created by the authors

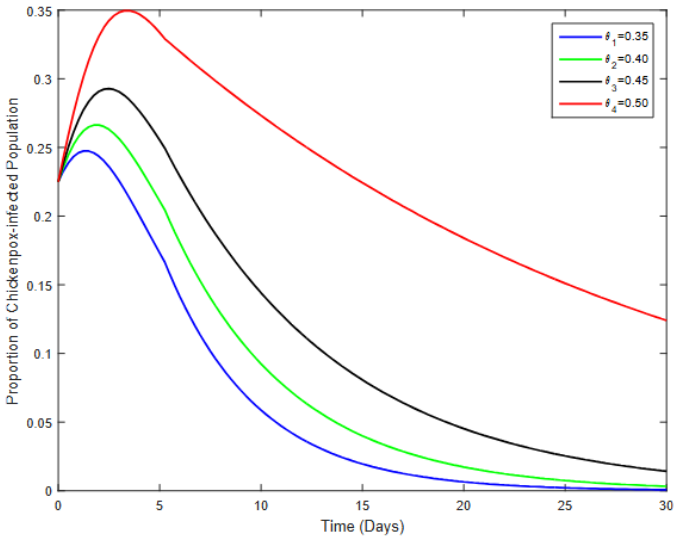


Fig. 5: Effect of vertical transmission rate θ on the proportion of chickenpox-infected individuals
Source: created by the authors

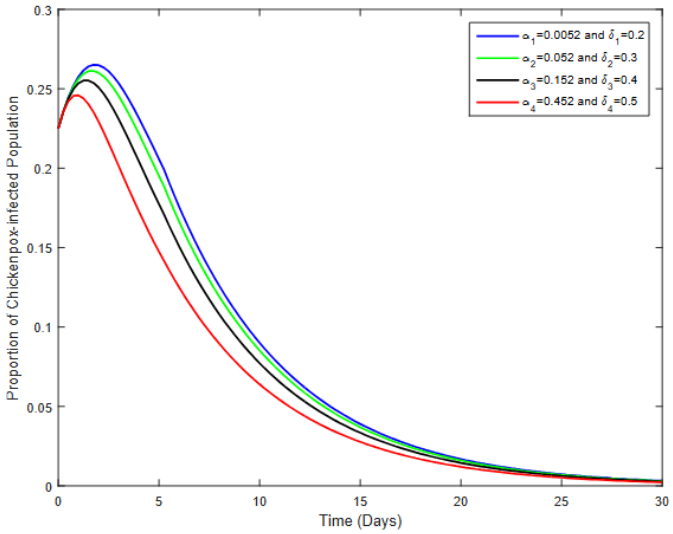


Fig. 6: Effect of first and second vaccination rates on chickenpox-infected individuals
Source: created by the authors

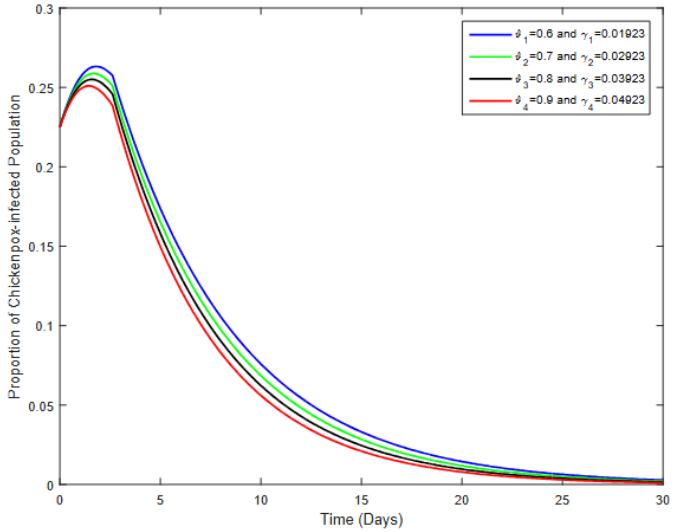


Fig. 7: Effect of treatment and recovery rates on chickenpox-infected individuals
Source: created by the authors